Polym. Bull. (2018) 75:3069–3087
https://doi.org/10.1007/s00289-017-2190-0

ORIGINAL PAPER

Investigation and fine-tuning of optoelectrical features of tertiary aminophenyl-activated poly(1,3,4-oxadiazole) conjugated system

Nimisha Kaippamangalath[1] · Unnikrishnan Gopalakrishnapanicker[1] · E. Shiju[2] · K. Chandrasekharan[2]

Received: 21 April 2017 / Revised: 13 July 2017 / Accepted: 19 September 2017 /
Published online: 5 October 2017

Abstract A novel π-conjugated polymer with *N*-alkyl substituted side chains, viz. poly[(2-*N*,*N*′-dibutylaminophenyl)1,3,4-oxadiazole] (PNAPO), possessing tunable optoelectronic properties, has been synthesized and characterized. PNAPO exhibited good solubility, indicating its suitability for easy optoelectronic device fabrication. Flexible films of PNAPO have been fabricated by adopting a blending route using poly(methyl methacrylate) or polystyrene. The effect of PNAPO particle size reduction, in the nanoregion, on the optical characterization was evaluated by a re-precipitation strategy. PNAPO has been found to exhibit an emission wavelength in the region of 522–590 nm with good quantum yield, for different particle size dimensions. Interestingly, it has been observed to exhibit solvatochromism. Z-scan experiments, with Nd:YAG laser, reveal that PNAPO possesses a low optical limiting threshold value. Interestingly, it shows a low turn-on voltage (0.23 V), suitable for fabricating the active layers in optoelectronic devices. PNAPO has been found to be stable up to 240 °C. These results highlight the possible utilization of PNAPO as an emissive layer in optoelectronic devices and for nonlinear optical (NLO) processes.

✉ Unnikrishnan Gopalakrishnapanicker
unnig@nitc.ac.in

Nimisha Kaippamangalath
nimisha.24387@gmail.com

E. Shiju
shijuhcu@gmail.com

K. Chandrasekharan
csk@nitc.ac.in

[1] Polymer Science and Technology Laboratory, Department of Chemistry, National Institute of Technology, Calicut, Kerala 673601, India

[2] Laser and Nonlinear Optics Laboratory, Department of Physics, National Institute of Technology, Calicut, Kerala 673601, India

Graphical abstract The graphical abstract represents the optical and electrical features of PNAPO. It indicates the structure of PNAPO. It shows the bright emissive property of PNAPO in the bluish green region of the electromagnetic radiation upon excitation with UV light. The light-emitting diode fabrication using PNAPO as an emissive layer is highlighted. A linear *I–V* characteristic of PNAPO has also been indicated through a current–voltage plot.

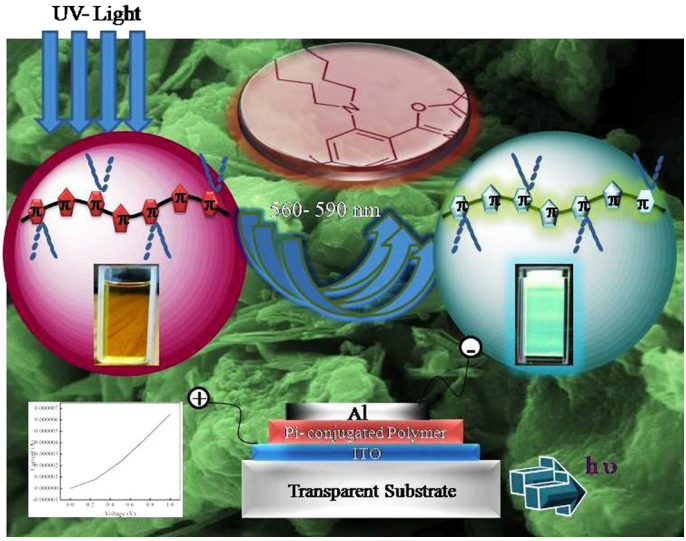

Keywords Polymeric material applications · Optical nanomaterials · Solvatochromism · Nonlinear optical effect · Fluorescence · Electrochemical properties

Introduction

π-Conjugated polymers have, by now, emerged as potential candidates for the fabrication of a variety of optoelectronic devices [1, 2]. The optical energy level, optical band gap, charge carrier mobility and solubility play crucial roles in their overall performance in the optoelectronic field. These features of π-conjugated polymers are highly sensitive to the backbone and substituent architectures. Obviously, altering the molecular architecture is an ideal strategy to modulate their optoelectrical properties.

Various classes of PCPs with impressive optoelectronic characteristics have been reported. Typically, Meng et al. [3] reported a π-conjugated system, having a carbazole moiety which is electron rich and an aromatic oxadiazole which is electron deficient in nature, as an attractive material for the development of polymer light-emitting diodes with high efficiency. Inagi et al. [4] investigated and tuned the optoelectronic properties of a series of PCPs containing triarylamine. Li et al.

demonstrated the design and synthesis of a soluble poly[2-methoxy-5-(3′-methoxy)butyl]-*p*-phenylenevinylene] (MMB-PPV), and the MMB-PPV films were implanted by nitrogen ion. The results showed that the ion implantation had a very important influence on the conductive property, optical absorption, optical band gap and the environmental stability of MMB-PPV film [5].

Among π-conjugated polymers, poly(1,3,4-oxadiazole) derivatives have been widely accepted by researchers for a spectrum of optoelectronic applications because of their electron-deficient nature, thermal resistance and high quantum yield [6–9]. Lee et al. [10] introduced a series of 1,3,4-oxadiazole containing π-conjugated macromolecules with adjustable optical and electrochemical properties. The emission spectra of these polymers were found to be in the red region of the electromagnetic spectrum. Huda and Dolui [11] studied photoluminescent properties of a series of soluble poly[1,3-bis(phenyl-1,3,4-oxadiazole)s] bearing polar groups in the main chain. Yang et al. [12] established new synthetic approaches for the preparation of copolymers of fluorene and oxadiazole with well-defined structures.

The disclosure of nonlinear optical (NLO) behaviour of polymers stimulated very interesting research programmes for the development of novel optical devices [13–15]. The examination of the nonlinear optical features of π-conjugated polymers, when exposed to high-intensity radiations, is a growing area of research. Various systems with significant optical nonlinearity have now been developed [16–19]. Conjugated polymers such as poly(thiophenes) and poly(fluorenes) are also reported to possess NLO activity along with an enhanced optical stability [20, 21]. These types of materials find wide applications in frequency modulators, electro-optical transducers, tunable interferometers and for surface-relief gratings useful for creating holograms and 3D images [22].

The major difficulties generally observed with many oxadiazole derivatives are low solubility for device fabrication and poor electrical conductance [23, 24]. Efforts are being done by various research groups to enhance these parameters along with an improvement in the fluorescence quantum yield. In this work, two butyl substituents linked to a phenylene ring in the chain have been introduced alternatively with 1,3,4-oxadiazole units to develop a new macromolecular architecture. Thus, we report a novel π-conjugated macromolecule having 1,3,4-oxadiazole and *N*,*N*′-dibutyl (side chains) activated phenylene units throughout the macromolecular chain (PNAPO). The linear optical properties and the electrochemical features have been investigated. The fine-tuning of the optical features has been achieved by a size reduction strategy using a re-precipitation method. The nonlinear optical responses of PNAPO have also been examined in a high-intensity laser (Nd: YAG) ambience.

Experimental section

Materials

The chemicals employed for the synthesis were of analytical grade and were purchased from Sigma-Aldrich, Bangalore, India.

Characterization

FT-IR spectra were obtained on a PerkinElmer Fourier transform infrared spectrometer (FT-IR), after pelletization with potassium bromide. The molecular weight was determined by gel permeation chromatography (GPC; Shimadzu, Japan) at 27 °C at a flow rate of 1 ml/min using DMF as eluent. The dimensions of nanosized aggregates were measured using a Malvern ZS Nano instrument at 25 °C. A PerkinElmer 3100 spectrophotometer was used to record absorption spectra in both solid and solution phases. Fluorescence spectra were carried out using a PerkinElmer LS 45 spectrofluorometer at an excitation wavelength $\lambda_{\text{abs max}}$ of the corresponding sample. The fluorescence quantum yield was calculated using quinine sulphate as the standard at an absorbance of 0.00115 with an integrated intensity of 3208. The Z-scan measurements for nonlinear responses were recorded on a standard open aperture Z-scan technique developed by Sheik-Bahae et al. [25]. A Q-switched, frequency-doubled Nd: YAG laser with 10 Hz repetition rate for excitation was employed for this purpose. The laser pulses possessed a pulse width of 7 ns at 532 nm wavelength. Thermogravimetric analysis (TGA) was carried out with a TGA Q50 V20.10 Build 36 from 0 to 800 °C at a heating rate of 10 °C/min under nitrogen atmosphere. In view of the easiness in product fabrication, the film forming ability of PNAPO was confirmed by mixing it with appropriate quantity of poly(methyl methacrylate)/polystyrene in DMF solvent, followed by casting. Cyclic voltammetry (CV) was performed on a CHI600D electrochemical workstation with a platinum working electrode and a Pt wire counter electrode at a scan rate of 50 mV/s against an $Ag/Ag^{+}(AgNO_3)$ reference electrode. The current–voltage characteristics of the samples were measured at room temperature using an Agilent B2902A precision source measure unit.

Results and discussion

Synthesis and characterization

The synthesis strategies towards the monomer and PNAPO are illustrated in Scheme 1. The dialkylation of aminoterephthalic acid using bromobutane was initially employed to obtain *N*,*N*′-dibutylaminoterephthalic acid. Dehydrocyclization reaction of the monomer, *N*,*N*′-dibutylaminoterephthalic acid, at 140–150 °C, subsequently produced the macromolecule, PNAPO with 65% yield. $M_n = 17{,}000$ g/mol, $M_w = 44{,}200$, PDI = 2.6.

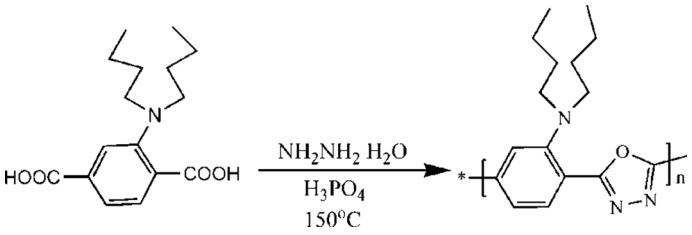

Scheme 1 Synthesis strategy for PNAPO

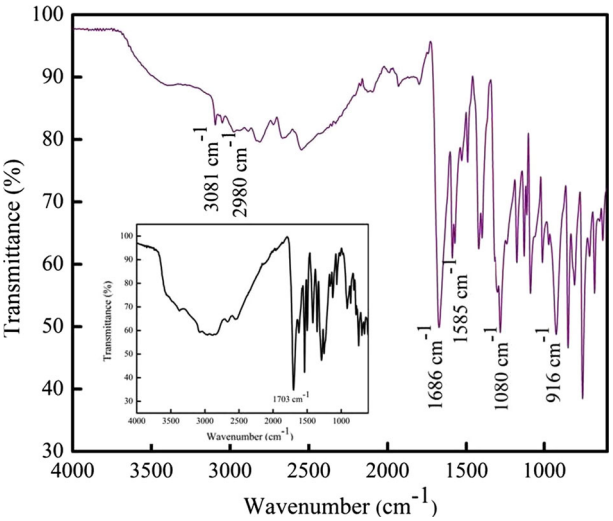

Fig. 1 FT-IR spectrum of PNAPO (FT-IR spectrum of *N*,*N*′-dibutylaminoterephthalic acid is shown in the inset)

IR spectrum of PNAPO is shown in Fig. 1.

In the FT-IR spectrum of PNAPO, shown in Fig. 1, peaks at 3081 and 2980/cm have been assigned to the aromatic and aliphatic C–H vibrations of PNAPO, respectively. In the FT-IR spectrum of the monomer, *N*,*N*′-dibutylaminoterephthalic acid (at the inset of Fig. 1), the broad peak at 3400/cm has been attributed to intermolecular or intramolecular hydrogen bonding. The observed disappearance of O–H stretching frequency in the spectrum of PNAPO can be considered as a strong evidence for the formation of the main macromolecular chain. In the FT-IR spectrum of the polymer, the absorption at 1686/cm can be attributed to the characteristic vibration of conjugated C=C. The strong absorptions at 1585 and 1080/cm are associated with the C=N and C–O–C stretching vibrations, respectively, of the oxadiazole unit. The stretching frequency at 916/cm further confirms the formation of 1,3,4-oxadiazole unit.

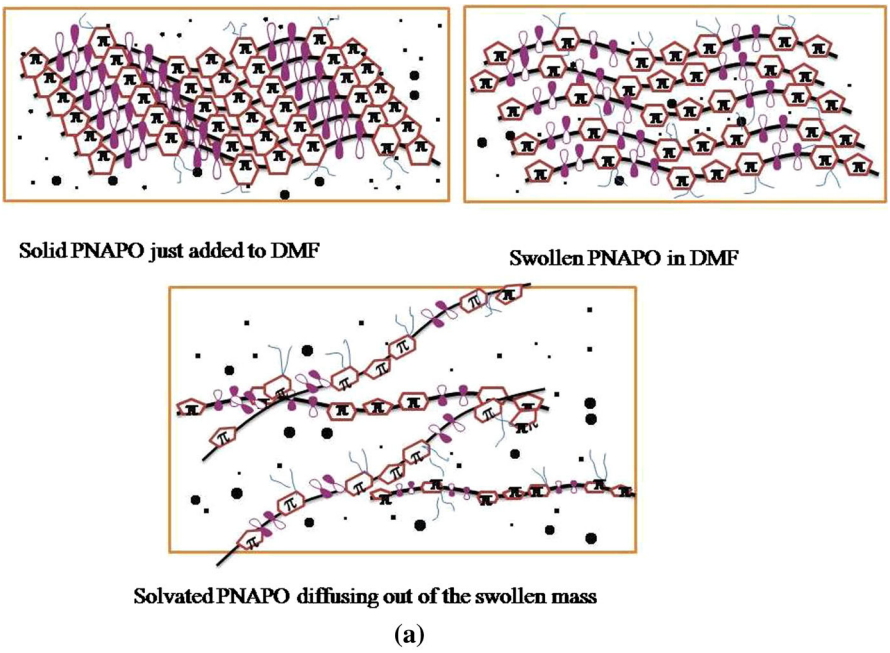

Scheme 2 Schematic representation for **a** dissolution of PNAPO in DMF, **b** film formation of PNAPO with PMMA/PS

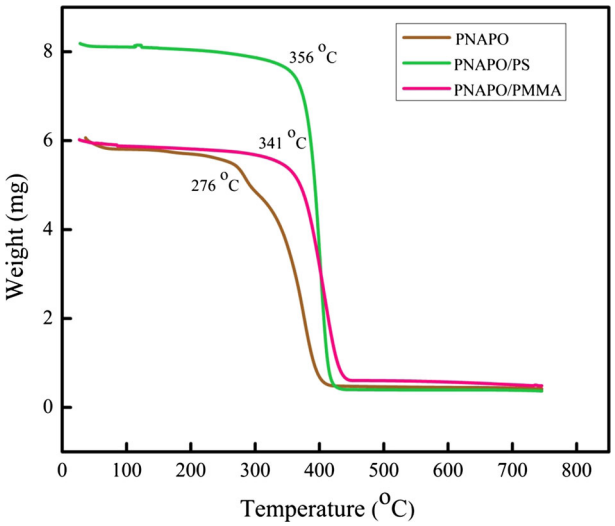

Fig. 2 Thermograms of PNAPO and PNAPO films with PMMA/PS

Solubility and film formation

PNAPO has been found to be soluble in formamide, DMF, methanol and THF. The solubility is accounted in terms of the lowering of the close packing of the main chains containing phenylene and oxadiazole units, by the introduction of long butyl side chains. This helps the penetration of solvent molecules effectively between the main chains and to enhance polymer–solvent interactions. In this way, the swelling, gelation and subsequent dissolution happen effectively. The dissolution processes of PNAPO in DMF are indicated in Scheme 2a.

The films of PNAPO can be formed on a glass substrate. However, for independent thin flexible film fabrication, a blending strategy has been explored using poly(methyl methacrylate) (PMMA) or polystyrene (PS) in DMF solvent. A fixed concentration of PMMA or PS (0.2 g/100 ml) in DMF has been found to be ideal to prepare polymer films with an average thickness of 55 μm. A representation of PNAPO film casting is given in Scheme 2b.

Thermal properties

Thermal stability is an important criterion for the use of any material as an active layer in optoelectronic devices. PNAPO showed stability up to 276 °C without any significant weight loss as shown in Fig. 2. Thermal stability has further been enhanced by blending with 0.2 wt% of PMMA/PS without scarifying the optoelectrical properties.

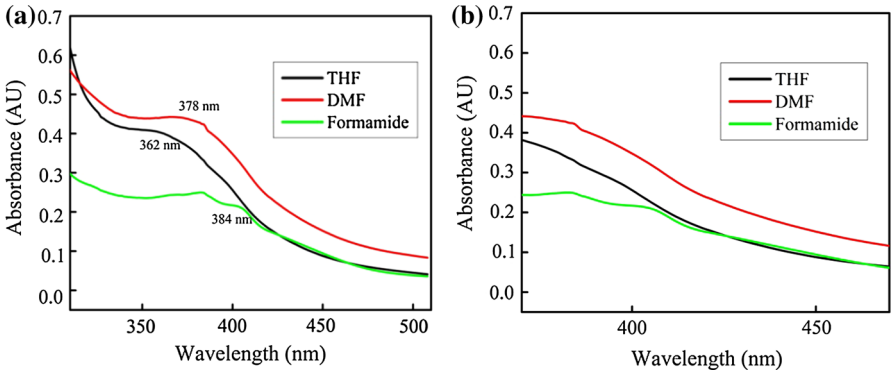

Fig. 3 **a** UV–vis absorption spectrum of PNAPO in different solvents, **b** absorption edges of PNAPO in different solvents

Photophysical properties

Photophysical properties of PNAPO were examined by means of UV–vis absorption and fluorescence analyses. Both UV–vis absorption and fluorescence spectra were observed in a range of organic solvents having different polarities.

UV–vis absorption spectra

PNAPO in DMF exhibits an absorption maximum ($\lambda_{\text{max abs}}$) of 384 nm assignable to the spin allowed π–π^* transition of π-electrons in the backbone of main macromolecular chains. It also indicates the high conjugation length of PNAPO. Depending on the polarity of the solvents (DMF, formamide and THF), there is a slight shift in the absorption maximum of the polymer, as shown in Fig. 3a. The band gaps (E_g) calculated for PNAPO from the absorption edges, 422, 414 and 407 nm for formamide, DMF and THF solutions (Fig. 3b), are 2.94, 2.99 and 3.04 eV using the formula, respectively [26]:

$$E_g = 1240/\lambda_{\text{edge}}, \tag{1}$$

where λ_{edge} is the value of onset absorption wavelength.

These optical band gap values promisingly offer the application of PNAPO as an active material in PLEDs [27].

Fluorescence spectra

The fluorescence spectra of PNAPO were recorded in DMF, formamide, THF and methanol and are shown in Fig. 4. The emission maximum of PNAPO in DMF is 552 nm, representing the green region of the electromagnetic spectrum. The related fluorescence quantum yield was computed using the formula [28]:

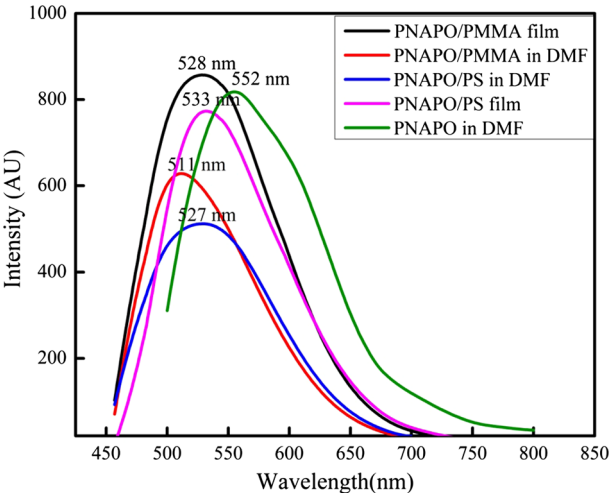

Fig. 4 Fluorescence spectra of PNAPO in solution phase and solid phase with PMMA/PS

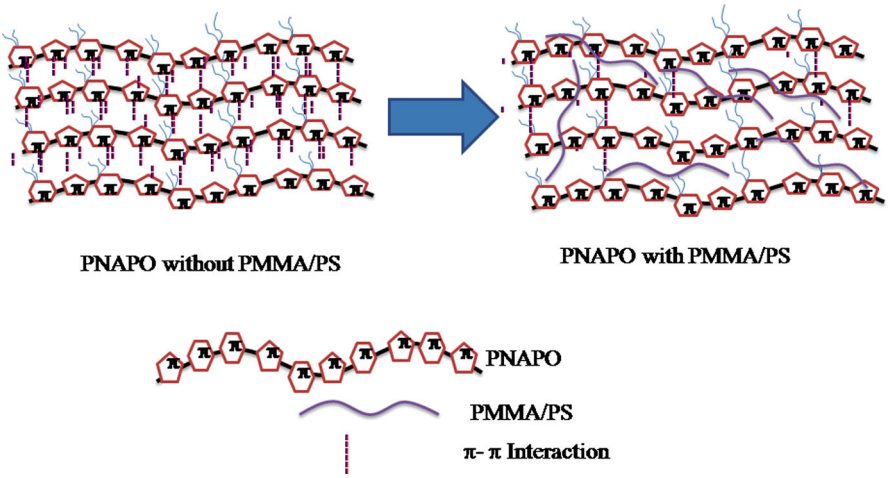

Scheme 3 π–π interaction between PNAPO macromolecules with and without PMMA/PS

$$QY_s = (Abs_{st}/Abs_s)\left(n_s^2/n_{st}^2\right)(I_s/I_{st})\,QY_{st}, \quad (2)$$

where Abs is the absorbance, n the refractive index, and I the integrated area under the fluorescence emission spectrum. The sub-indices s and st correspond to the PNAPO and the standard (quinine sulphate), respectively. The fluorescence quantum yield for PNAPO has been found to be 28%. This high quantum yield value indicates a lesser π–π stacking between the main macromolecular chains due to the presence of long butyl side chains attached to the main backbone [29, 30]. This

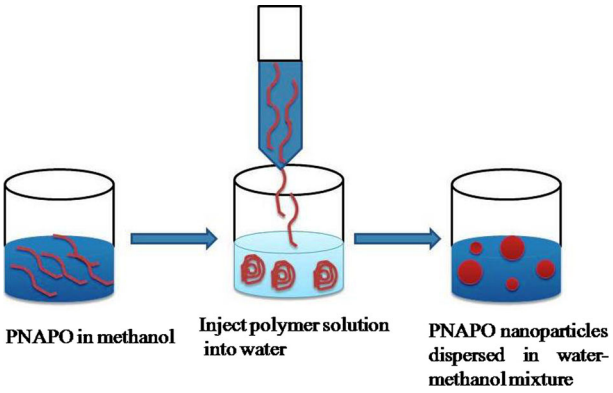

Scheme 4 Schematic representation of re-precipitation method [31]

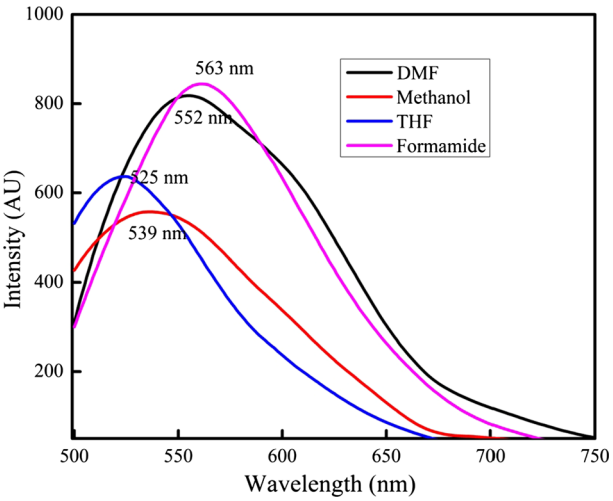

Fig. 5 Effect of solvents on the emission maximum of PNAPO

obviously highlights the possibility of fabricating emissive layers in green light-emitting optoelectronic devices, using PNAPO.

The systems, PNAPO with either PMMA or PS, in solution phase are also found to be bright fluorescent in the bluish green region of the electromagnetic spectrum (Fig. 4). A slight blue shift has been observed in the emission maximum of the blended form. This is mainly due the minimization of π–π interactions of the main macromolecular chains of PNAPO (Scheme 3). The red shift of the emission maxima for PNAPO, with PMMA/PS, films in solid state compared to solution phase is due to the more effective π–π stacking of the former in the solid phase. However, all the blended forms, i.e. both solution and film forms phases, are slightly blue-shifted compared to that of PNAPO alone in DMF (Scheme 4).

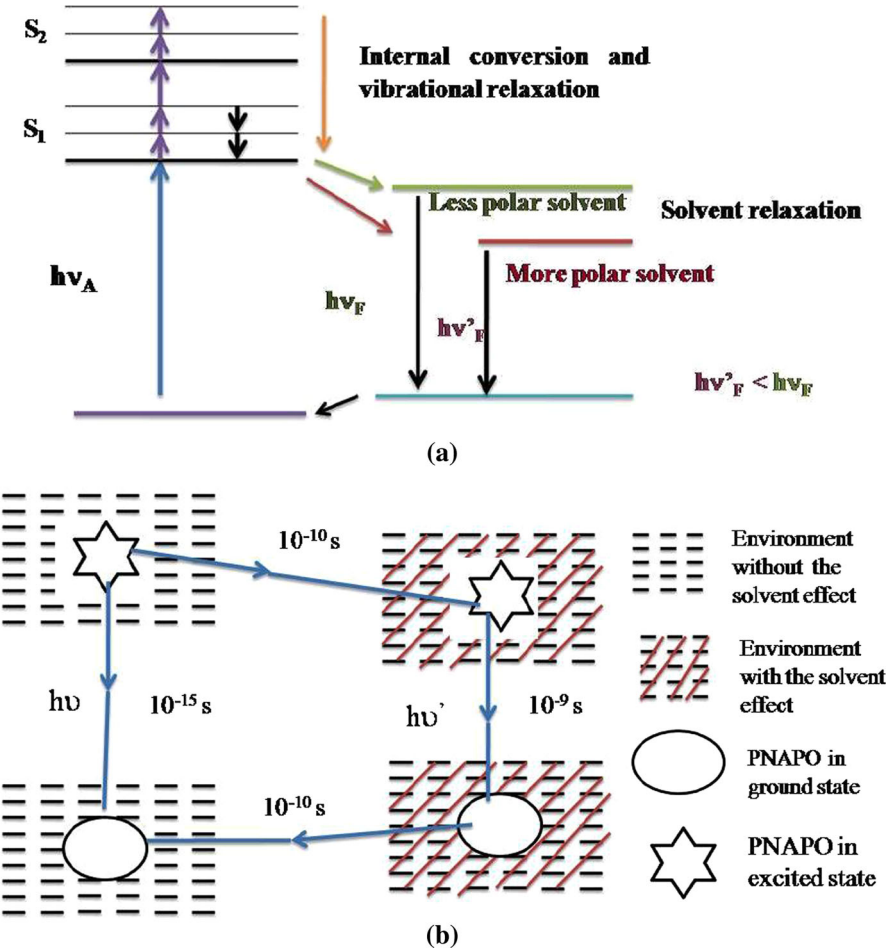

Fig. 6 Schematic illustration for **a** energy level diagram and **b** environmental effect of solvent for solvatochromism [28]

Solvatochromism

Solvatochromism, the shift in the emission wavelength with change in polarity of the solvents, of PNAPO was examined in four solvents, viz. DMF, formamide, methanol and THF. Figure 5 depicts the effect of solvents on the emission maximum (λ_{max}) of PNAPO. It is seen that the λ_{max} is in the order: formamide > DMF > methanol > THF. These characteristics can be attributed to two factors. The electron cloud expands on electronic excitation, which typically increases the polarizability (change of polarity by extrinsic fields) and lowers the excitation energy. Secondly, the process of electronic excitation takes place within approximately 10^{-15} s, while the reorientation of the nuclei and the solvent

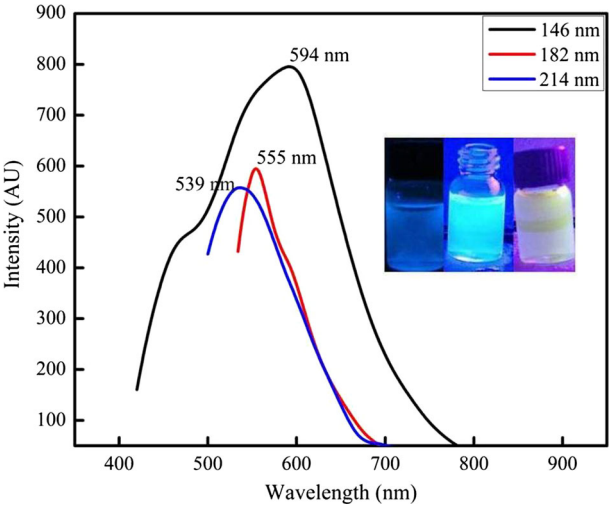

Fig. 7 Effect of size reduction on the emission maximum of PNAPO in methanol

molecules takes much longer time (approximately 10^{-10} s, Frank–Condon principle) as indicated in Fig. 6.

As shown in Fig. 6a, after excitation, PNAPO can reach the excited state in a polar medium due to dipole–dipole interactions. A more polar environment can lead to a more stabilized system with a lower energy. As shown in Fig. 6b, normally the molecule after excitation returns to the ground state in 10^{-15} s. However, when solvents of high polarity are employed, the excited state gets stabilized, typically for 10^{-10} s. Subsequent slightly delayed return to the ground state, through a relaxed excited state, results in the emission of lower energy or higher wavelength. Thus, the emission spectrum of PNAPO in DMF is more red-shifted than those of PNAPO in formamide, methanol and THF.

Fine-tuning of optical properties

In our recent experiments with a π-conjugated system, viz. poly(2-nitro-phenylene-1,3,4-oxadiazole) (PNPO), we observed a significant change in the emission features with a change in its particle size in solution phase [31]. A re-precipitation technique, as shown in Scheme 4, was employed for the effective size reduction of the macromolecular chains [32]. Similarly, a dropwise addition of PNAPO in methanol into the poor solvent, water, with stirring under ultrasonication was done to generate polymer chains of reduced dimensions. Various dimensions of nanosized aggregates were obtained simply by adjusting the concentration of PNAPO in methanol. The mean particles sizes of the nanoaggregates, evaluated by dynamic light scattering, have been found to be 146 and 182 nm, respectively, for 0.002 and 0.001 g/ml concentrations of PNAPO.

The effect of the reduced size of PNAPO on the emission features is illustrated in Fig. 7. It is seen that, as the size of PNAPO decreases, the emission becomes red-

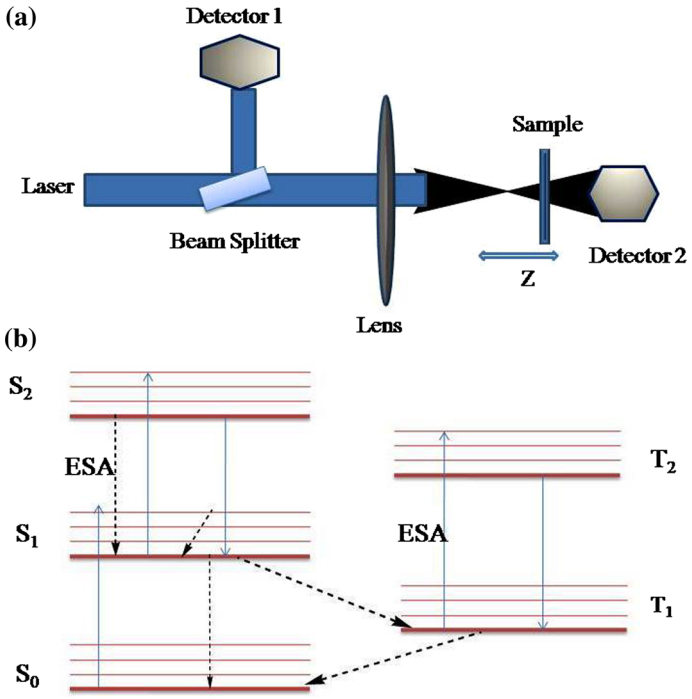

Fig. 8 **a** Z-scan set-up and **b** five-level energy model

shifted. This is obviously due to strong intermolecular π–π interactions of polymer chains in the aggregated form [33].

Nonlinear optical (NLO) properties

The Z-scan set-up used for the investigation of nonlinear optical (NLO) properties of PNAPO is given in Fig. 8. A five-level model [32] describing the NLO mechanism of π-conjugated polymers is also shown in this figure.

In the model, S_0 represents the ground state, while S_1 and S_2 are the first and second excited states, respectively. T_1 and T_2 are the first and second triplet excited states, correspondingly. Excitation of the molecule from the ground state S_0 to the first excited singlet state S_1 occurs by the absorption of two photons simultaneously, when the molecule is irradiated with a 532 nm, 7 ns pulses. There is a chance for the further excitation of the molecule to the upper state S_2. The singlet transition does not dry up the population in S_1, because the decay from S_2 to S_1 happens in the order of picoseconds. In spite of that, they can be transferred from S_1 to a lower triplet state T_1 through a spin flip transition called intersystem crossing from where excitation to a higher triplet state T_2 can occur.

Figure 9a–c represents the open aperture (OA) Z-scan traces of PNAPO (original and reduced dimensions) in DMF solvent, with normalized transmittance plotted against position of the sample with respect to the laser beam. Optical limiting curves

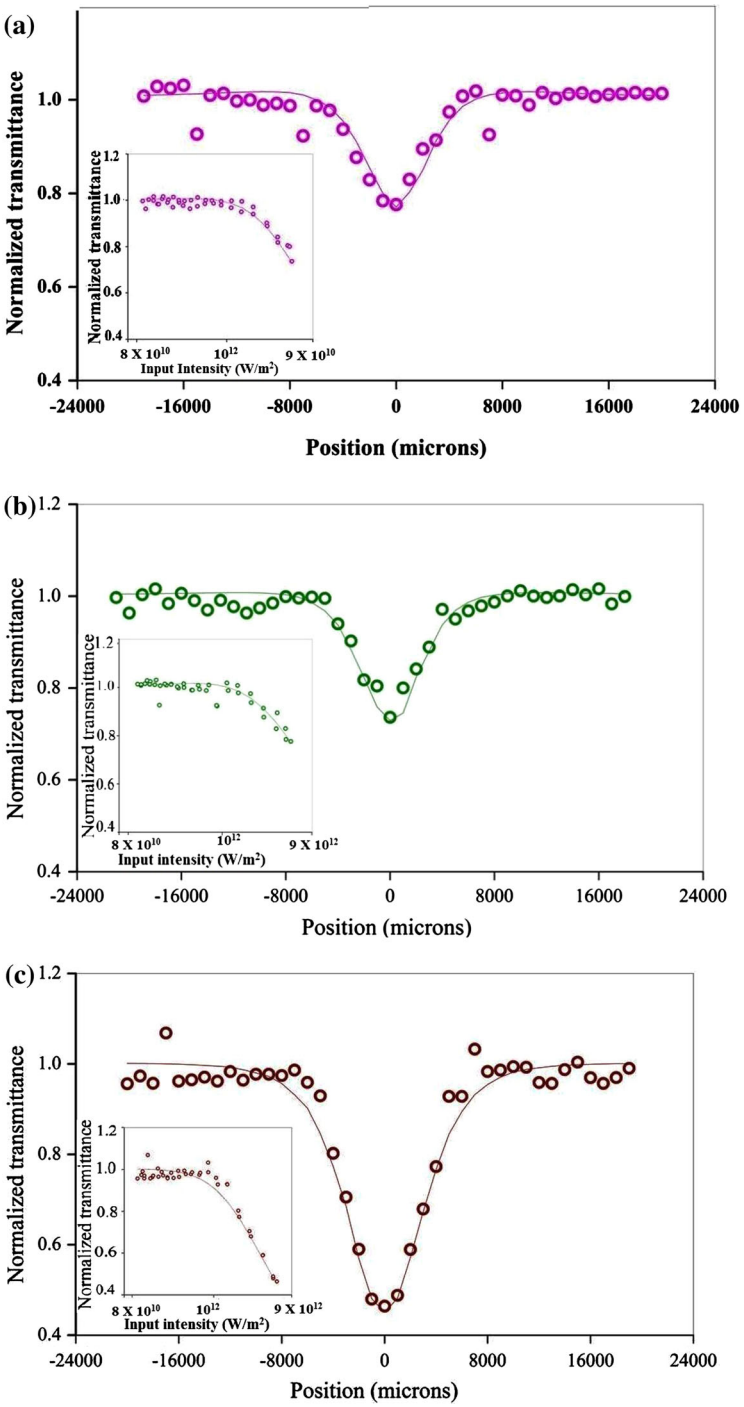

Fig. 9 Nonlinear responses of PNAPO **a** 214 nm, **b** 182, **c** 146 in DMF

of each sample, extracted from the Z-scan data, are shown at the inset of each figure (Fig. 9a–c), where the normalized sample transmittance is plotted against the input laser fluence. It is seen that the curves start deviating from the conventional Beer's law of linear dependence after a threshold laser intensity. In a real-time experiment, the solution turns to be opaque at this point, leading to optical power limiting, the nonlinear process.

The optically induced polarization in a material by the interaction with light can be described as a power series in the electric field as shown in Eq. 3 [33]:

$$A = \chi^{(1)}.E + \chi^{(2)}.E.E + \chi^{(3)}.E.E.E + \cdots, \tag{3}$$

where the expansion coefficients (χ) are known as the first-, second- and third-order susceptibilities, respectively.

There exists a similar relationship between the dipole moment of a molecule and the electric field [Eq. 4]:

$$A = \alpha.E + \beta.E.E + \gamma.E.E.E + \cdots, \tag{4}$$

where α is the polarizability, β the hyperpolarizability, and γ the second hyperpolarizability of the molecule.

Larger the molecular hyperpolarizability, higher the number of dipole moment necessary in order to achieve a large NLO effect. The nonlinear absorption coefficient, β, for PNAPO was obtained by fitting the experimental scan plot of the open aperture measurement to Eq. 5 [34].

$$T(z) = \frac{C}{q\sqrt{\pi}} \int_{-\infty}^{\infty} \ln\left(1 + q_0 e^{-r^2}\right), \tag{5}$$

where $q_{(z,r,t)} = \beta I(\alpha t) L_{\text{eff}}$ and $L_{\text{eff}} = (1-\mathrm{e}^{-l})/\alpha$ is the effective thickness with the linear absorption coefficient, α and I is the irradiance at the focus.

The third-order nonlinear susceptibility, $\chi^{(3)}$, was calculated using Eq. 6 [35]:

$$\chi^{(3)} = \left(n_0^2 \varepsilon_0 C \lambda \beta / 2\pi\right)/1.4 \times 10^{-8}, \tag{6}$$

where n_0 is the refractive index, ε_0 is the permittivity, C is the velocity of the light, λ

Table 1 Nonlinear optical responses of PNAPO

Size (nm)	Refractive index (n)	Nonlinear absorption coefficient (β) 10^{-10}	Linear transmission	$\chi^{(3)}$ (esu)
PNAPO				
214	1.42	1.07	0.7	3.46×10^{-12}
182	1.415	1.65	0.64	5.3×10^{-12}
146	1.42	4.2	0.6	1.32×10^{-11}

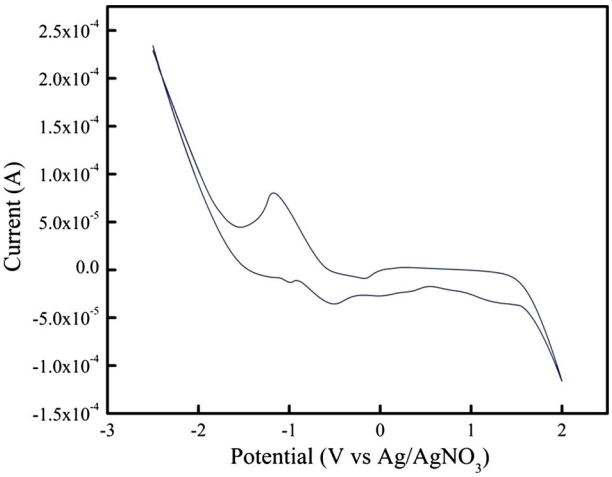

Fig. 10 Cyclic voltammogram of PNAPO

is the wavelength of the light, and β is the nonlinear absorption coefficient of sample solution.

The calculated third-order nonlinear susceptibilities, $\chi^{(3)}$, of PNAPO of different sizes are listed in Table 1. The $\chi^{(3)}$ values have been found to be increased with a reduction in size. This shows that the NLO responses get enhanced when the size is reduced. This can be viewed in terms of reduction in energy level gaps with a reduction in particle size of the macromolecules in solution phase. Alternatively, a particle size reduction leads to a better optical limiting performance. In view of the above observations, PNAPO has been proposed as a promising candidate for the

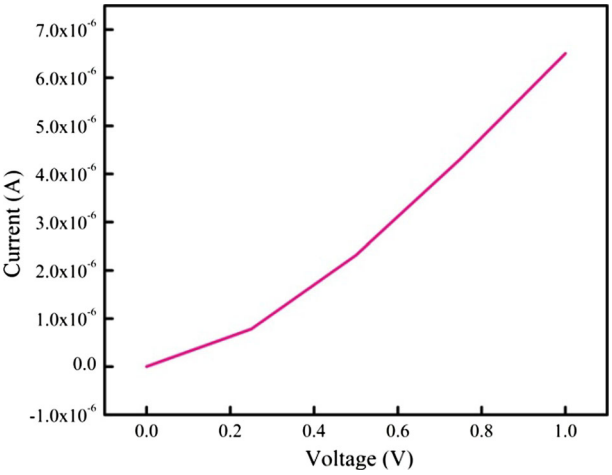

Fig. 11 Current–voltage characteristics of PNAPO

fabrication of active layers in polymer light-emitting diodes. The graphical abstract indicates the utilization of PNAPO in PLEDs.

Electrochemical properties

The redox behaviour of PNAPO was examined by cyclic voltammetry in DMF solvent using tetrabutylammonium perchlorate (TBAPC) (0.1 M) as an electrolyte, Pt as the working electrode and Ag/Ag^{+} ($AgNO_3$) as the reference electrode at a scan rate of 50 mV/s. The HOMO and LUMO energy levels were estimated from the onset oxidation and reduction potentials (Fig. 10) using the Eqs. 7a and 7b [36, 37].

$$E_{\mathrm{HOMO}} = -\left[E^{\mathrm{OX}}_{(\mathrm{onset})} + 4.8\ \mathrm{eV}\right], \tag{7a}$$

$$E_{\mathrm{LUMO}} = -\left[E^{\mathrm{Red}}_{(\mathrm{onset})} + 4.8\ \mathrm{eV}\right]. \tag{7b}$$

The calculated HOMO and LUMO energy levels of PNAPO are − 6.26 and − 3.29 eV, respectively, and the band gap is 2.96 eV. This value is comparable with the band gap calculated from the absorption edge (2.99 eV).

Figure 11 shows the current vs. voltage relation of a uniformly coated PNAPO glass substrate. PNAPO has been found to possess a turn-on voltage of 0.23 V. This low turn-on voltage of PNAPO is due to the high π-electron delocalization throughout the main macromolecular system derived through the activation effect of butyl-substituted phenylene ring on 1,3,4-oxadiazole unit, a hole-transporting entity in the main chain and a high conjugation length. This observation on the electrical properties also supports the proposal for utilizing PNAPO as active layers in PLEDs.

Conclusions

A new π-conjugated polymer, viz. poly[(2-*N*,N′-dibutylaminophenyl)1,3,4-oxadiazole] (PNAPO) with interesting optoelectrical features, has been synthesized and characterized. PNAPO showed excellent solubility in a range of organic solvents indicating the easiness in processability. The modulation of optical properties was achieved by size reduction using a re-precipitation technique. For the commercial application of PNAPO, homogenous film fabrication was confirmed via a blending strategy using 0.2 wt% of PMMA or PS in DMF solvent. The investigations of the absorption and emission features strongly proposed the utilization of PNAPO as an emissive source in optoelectronic devices, especially in PLEDs, in the bluish green or green region of the electromagnetic spectrum. PNAPO showed polarity-dependent emission features in four organic solvents having different polarities. The observed NLO features of PNAPO have been found to be ideally suitable for optical switching and limiting technologies.

Acknowledgements NK gratefully acknowledges financial support from Council of Scientific Research (Council of Scientific and Industrial Research, New Delhi, India) fellowship in Chemical Sciences.

References

1. Yang Y, Guanxin Z, Hewei L, Jingjing Y, Zitong L, Deeqing Z (2016) Highly sensitive thin film field effect transistor for ammonia with DPP-bithiophene conjugated polymer entailing thermally cleavable tert-butoxy groups in the solid chains. ACS Appl Mater Interfaces 8:3635–3643
2. Kakaraparthi K, Sang HP, Woosum C, Won-TP Yong-YN, Sung-HJ Jae WL (2016) New bulky side chain substituted benzodithiophene based 2D-conjugated polymers for optoelectronic applications. Polym Bull 73:2567–2581
3. Meng H, Zhi KC, Xiao LL, Yee HL, Soo JC, Wei H (1999) Synthesis and characterization of a novel blue electroluminescent polymer constituted of alternating carbazole and aromatic oxadiazole units. Phys Chem Chem Phys 1:3123–3127
4. Inag S, Noriyuki K, Shotaro H, Toshio F (2014) Facile synthesis of a variety of triarylamine-based conjugated polymers and tuning of their optoelectronic properties. Synth Met 187:81–85
5. Li B, Lei C, Yuying Z (2010) Conductive and optical properties of PPV modified by N^+ ion implantation. J Polym Sci Part B Polym Phys 48:2072–2077
6. Bogdan Z, Yuriy B, Volodymyr T, Christopher FH, Jamie AS, Parul R, Ryan DR, Charles T, Stephen EC, Stephen HF (2015) Rational design of methacrylate monomers containing oxadiazole moieties for single-layer organic light emitting devices. J Polym Sci Part B Polym Phy 53:1663–1673
7. Shuhei Y, Seijung P, Suhee S, Mihee H, Joo YS, Youngeup J et al (2010) Synthesis and characterization of fluorene-carbazole and fluorene-phenothiazine copolymers with carbazole and oxadiazole pendants for organic light emitting diodes. Polymer 51:6174–6181
8. Huajie C, Hui H, Zongfang T, Ping S, Bin Z, Songting T (2010) Synthesis and photovoltaic erformances of 2,5-dioctyloxy-1,4-phenylenevinylene and terthiophene copolymers with di(p-tolyl)phenylamine and oxadiazole side groups. Eur Polym J 46(2010):673–680
9. Nam CY, Seok C, Dong HS (2003) Synthesis and optically acid-sensory properties of novel polyoxadiazole derivatives. Polymer 44:2143–2148
10. Lee K, Hyong-JK Jae CC, Jinsang K (2007) Chemically and photochemically stable conjugated poly(oxadiazole) derivatives: a comparison with polythiophenes and poly(*p*-phenyleneethynylenes). Macromolecules 40:6457–6463
11. Huda MK, Dolui SK (2010) Luminescence property of poly(1,3-bis(phenyl-1,3,4-oxadiazole))s containing polar groups in the main chain. J Lumin 130:2242–2246
12. Yang NC, Chang IL, Jong KK, Dong HS (2004) Dependence of optical properties on the preparation methods of poly[(9,9′-dialkylfluorene- 2,7-diyl)-*alt*-(1,3,4-oxadiazole-2,5-diyl)]. J Appl Polym Sci 92:3112–3118
13. Marks TJ, Ratner MA (1995) Design, synthesis and properties of molecule- based assemblies based with large second-order optical nonlinearities. Angew Chem Int Ed Engl 34:155–173
14. Heddi M, Guy CB, Gary DP (1996) The effects of surface layers on third harmonic generation from solution of nematogenic polymer. J Polym Sci Part B Polym Phys 34:925–938
15. Zhongan L, Gui Y, Zhen L, Yunqi L, Cheng Y, Jingui Q (2008) New second order nonlinear optical polymers containing the same isolation groups: optimized syntheses and nonlinear optical properties. Polymer 49:901–913
16. Sona N, Anshad A, Sreejesh PR, Krishnapillai S, Cheranellore SK, Rani J (2015) Theoretical and experimental investigations on the photoconductivity and nonlinear optical properties of donor-acceptor pi-conjugated copolymer, poly(2,5-(3,4-ethylenedioxythiophene)-*alt*-2,7-(9,9-dioctylfluorene)). RSC Adv 5:8657–8668
17. Chao G, Shaojun Q, Weisong D, Qun L, Hongcai W, Xiaozeng L, Hongyan G (2010) Enhanced third-order nonlinear optical property of poly(3-decayl)thiophene films modified by N^+ ion implantation. Synth Metal 160:2175–2179
18. Bass M, Enoch JM, Van Stryland EW, Wolfe WL (2001) Handbooks of optics IV-fiber optics and nonlinear optics. McGraw-Hill, New York
19. Guo Y, Kao CK, Li EH, Chiang KS (2002) Nonlinear photonics. Springer, Berlin
20. Massimiliano L, Luisa P (2009) New photosetting NLO^- active thiophenes with enhanced optical stability. Eur Polym J 45:1118–1126

21. Wenbo W, Qi H, Cheng Z, Cheng Y, Jingui Q, Zhen L (2013) Second-order nonlinear (NLO) optical polymers containing perfluoroaromatic rings as isolation groups with Ar/Ar^{F} self-assembly effect: enhanced NLO coefficient and stability. Polymer 54(2013):5564–5655
22. Ru S, Yue-TL Bao-LY, Jian-ML Xing-ZW, Ying-LS Jian-FG (2014) Third-order nonlinear optical properties of the poly(methyl methacrylate)-phenothiazinium dye hybrid thin films. Thin Solid Films 551:153–157
23. Jainez Anlauf S, Wedel A (2001) New n-type rigid rod full aromatic poly(1,3,4-oxadiazole)s and their application in organic devices. Synth Metal 122:11
24. Michael G, Peter S, Martin M, Wolfgang B (1997) Polymethacrylate with pendant oxadiazole units synthesis and application in organic LEDs. Macromolecules 30:6042–6046
25. Hutchings DC, Sheik-Bahae M, Hagan DJ, Van Stryland EW (1992) Kramers-Kronig relation in nonlinear optica. Opt Quantum Electron 24:1–30
26. Bayram G (2015) Optical properties of poly[2-methoxy-5-(3′-dimethyloctyloxy)-1,4-phenylenevinylene] light-emitting polymer solutions: effects of molarities and solvents. Polym Bull 72:3241–3267
27. Joo HK (2008) Synthesis and electro-optical properties of poly(*p*-phenylenevinylene) derivative with conjugated 1,3,4-oxadiazole pendant and its AC electroluminescence. Synth Metal 158:1028–1036
28. Joseph RL (2006) Principles of fluorescence spectroscopy. Springer, Baltimore
29. Hensema ER, Sena MER, Mulder MHV, Smolders CA (1994) Synthesis and properties of related polyoxadiazoles and polytriazoles. J Polym Sci Part A Polym Chem 32:527–537
30. Jianfu D, Micheal D, Gilles R, Jacques R (2005) Synthesis and characterization of alternating copolymers of fluorene and oxadiazole. Macromolecules 32:3474–3483
31. Nimisha K, Shiju E, Chandrasekharan K, Unnikrishnan G (2016) Synthesis, characterization, and fine tuning of optical properties of soluble π-conjugated system with nito-phenyl-activated 1,3,4-oxadiazole unit. J Mater Sci 51:4748–4761
32. Landfester K (2009) Miniemulsion polymerization and the structure of polymer and hybrid nanoparticles. Angew Chem Int Ed 48:4488–4507
33. Sahan DP, Stephen GU (2017) Systematic investigation of π–π interactions in near edge X-ray fine structure (NEXAFS) spectroscopy of paracyclophanes. J Phys Chem A. doi:10.1021/acs.jpca.7b03823
34. Tiziana C, Raffaele T, Andrew PM, Micheal DW (2005) Investigation of the excited state absorption of a Ru dioxoline complex by the Z-scan technique. J Chem Phys 122:154507–154512
35. Saadeh H, Yu D, Wang LM, Yu LP (1999) Highly stable, functionalized polyimides for second order nonlinear optics. J Mater Chem 9:1865–1873
36. Sona N, Sreejesh PR, Aby CP, Sebastian M, Krishna PS, Cheranellore SK, Rani J (2015) Third-order nonlinear optical properties of 3,4-ethylenedioxythiophene copolymers with chalcogenadiazole acceptors. New J Chem 39:2795–2806
37. Mengxia L, Wen W, Luying L, Shuhui Y, Qidan L (2017) Synthesis of D-A low-bandgap polymer-based thieno[3,4-*b*]pyrazine and benzo[1,2-b:4,5-*b*′]dithiophene for polymer solar cells. Polym Bull 74:603–614